

Photochemistry of Salicylaldoxime in Solid Argon: An Experimental and Theoretical Study

Joanna Grzegorzek^[a] and Zofia Mielke^{*[a]}

Keywords: Oximes / Photochemistry / Isomerization / Matrix isolation / Density functional calculations

The photochemistry of salicylaldoxime in solid argon has been investigated by FTIR spectroscopy and DFT calculations. The salicylaldoxime molecule trapped in the matrix from the vapor above the solid sample has the most stable *syn1* conformation with an intramolecular hydrogen bond. Irradiation ($\lambda > 320$ nm) leads to conversion of the *syn1* conformer into the *syn3* one, in which the C(H)NOH and (C)OH groups are rotated around the C–C and C–O bonds, respectively, and the intramolecular hydrogen bond is broken. The photochemistry of *syn3* involves three possible routes: (i) conversion of *syn3* into *anti2* conformer, this process requires rearrangement of the NOH group with respect to the

C=N bond; (ii) photodissociation of salicylaldoxime into 2-cyanophenol and water, which form a hydrogen-bonded complex; and (iii) regeneration of the *syn1* conformer. The third route is a very small contribution to the overall process. The study performed with [D₂]salicylaldoxime indicates that the dehydration reaction of salicylaldoxime involves cleavage of the N–O bond and formation of OH and Ph(OH)C(H)N radicals in the first step. Then, the OH radical abstracts a hydrogen atom from the CH group to form 2-cyanophenol and water molecules. When the sample is exposed to the full output of the mercury lamp the 2-cyanophenol complex with water becomes the dominating product.

Introduction

Oximes constitute an important and very interesting class of organic compounds owing to their ambifunctional nucleophilic properties. They have found wide application in synthetic organic chemistry^[1] mainly as protecting groups for carbonyl compounds. Many oximes are used as agricultural chemicals^[2] and in pharmacology as antidotes for organophosphorous poisoning.^[3–6] They are also considered to be potential source of NO in living organisms.^[7,8]

The photochemical reactions of oximes have received considerable attention.^[9–14] The three most important reactions resulting in excitation of the C=N bond are isomerization, rearrangement, and hydrolysis. Photoinduced *syn–anti* (or *anti–syn*) isomerization reactions in oximes are among the first photoreactions ever described. The photoisomerization reactions of aromatic oximes have been studied by several groups;^[15] the infrared spectra of *syn* and *anti* isomers of benzaloxime in solid argon and nitrogen have been recently reported.^[14] Irradiation of oximes may also induce the photo-Beckmann rearrangement reaction that results in the formation of amides or carbonyl compounds.^[16]

Haley and Yates investigated thoroughly the photochemistry of aromatic oximes subjected to radiation at $\lambda = 254$ and 300 nm.^[17,18] They found that both aromatic aldoximes

and ketoximes undergo photohydrolysis through their lowest singlet state (with relatively low quantum yield), yielding the corresponding carbonyl compound.

Some *syn–anti* isomerization was also observed and was suggested to occur from the lowest triplet excited state.^[17] The photochemistry of *o*-hydroxy-substituted aromatic oximes in aqueous solutions exposed to 350, 300, and 254 nm radiation has also been reported.^[18–20] The major result of photolysis of salicylaldoxime was cyclization to give benzoxazole; however, photohydrolysis producing salicylaldehyde was found to be competitive with cyclization, especially in acidified solutions.^[18] In irradiated aqueous base solution of salicylaldoxime some amount of 2-cyanophenol and a trace amount of salicylaldehyde were identified in addition to the cyclization photoproduct benzoxazole.^[19]

Haley and Yates^[18] suggested the mechanism of the cyclization reaction of salicylaldoxime. On the basis of the fluorescence emission and excitation spectra of salicylaldoxime the authors put forward a hypothesis on the existence of two major ground-state conformers of the molecule, one having an intramolecular hydrogen bond and the other being hydrogen bonded to the solvent. The population of the two conformers was dependent on the solvent; in water and in solvents capable of strong hydrogen bonding, the conformation with an intermolecular hydrogen bond was stabilized, whereas in nonpolar solvents like pentane and cyclohexane the conformer with an intramolecular hydrogen bond was also populated. The cyclization reaction was believed to occur by two different mechanisms, arising from the inter- and intramolecularly hydrogen-bonded conform-

[a] Faculty of Chemistry, Wrocław University, 14, F. Joliot-Curie, 50-383 Wrocław, Poland
Fax: +48-71-3282-348
E-mail: zm@wchuwr.pl

Supporting information for this article is available on the WWW under <http://dx.doi.org/10.1002/ejoc.201000348>.

ers, respectively. One mechanism was proposed to involve cyclization via the phenolate ion, whereas the other one was believed to involve intramolecular proton transfer to give a zwitterionic intermediate. The conformational studies of salicylaldehyde in $[D_6]DMSO$ have been performed by help of ^{13}C NMR spectroscopy.^[21,22] In an earlier report^[21] the authors claimed that there is a mixture of the “free” and “intramolecularly hydrogen-bonded” forms of salicylaldehyde in $[D_6]DMSO$, whereas the more recent study^[22] resulted in the presence of the latter conformer only.

There has been recently a renewed interest in the chemistry of salicylaldehyde and its derivatives^[23–27] owing to their application in synthetic chemistry, among others in the synthesis of benzoxazole.^[23] There are still many questions concerning the photochemical behavior of salicylaldehyde and up to now the infrared spectra of its conformers have not been characterized. We performed the study of the photochemistry of salicylaldehyde by help of the matrix isolation technique coupled with infrared spectroscopy. Matrix isolation has proved to be an extremely powerful technique in conformational studies^[28] and in the identification of reaction intermediates.^[29]

Results and Discussion

Photochemistry of Salicylaldehyde

Figure 1 presents various spectral regions of the argon matrix doped with salicylaldehyde. The spectra were recorded directly after matrix deposition and after its irradiation

with $\lambda > 320$ nm followed by irradiation with the full output of the mercury lamp. As one can see, the bands observed in the spectra recorded directly after matrix deposition (Figure 1, marked S1) strongly diminish during irradiation, whereas new bands start to appear. These new features can be divided into three groups (Figure 1, marked S3, A2, and C) on the basis of their response to exposure of the matrix to the mercury lamp radiation. Absorptions in a particular group exhibited a constant relative intensity through a single experiment and between different experiments and may, therefore, be associated with the same species. In Figure 2 time evolution of salicylaldehyde (S1) and photoproducts (S3, A2, and C) in a salicylaldehyde/argon matrix after its exposure to $\lambda > 320$ nm radiation is presented. During the first 10 min of matrix irradiation, photoproduct S3 is formed at the expense of salicylaldehyde S1, and the yield of photoproducts A2 and C is very small. During the next 70 min, the concentration of S3 decreases, whereas the concentrations of A2 and C increase. When the matrix is photolyzed with the full output of the mercury lamp photoproduct C grows at the expense of S3 and A2. A very small amount of S1 is present in the matrix even after a long irradiation time.

In Table 1 the frequencies of the most intense absorptions characteristic for salicylaldehyde S1 and for photoproducts S3 and A2 are collected; the full sets of frequencies identified for S1, S3, and A2 are presented in the Supporting Information (Tables S2–S4). Many bands characteristic for S1, S3, and A2 appear at very close frequencies, which suggests that they correspond to three dif-

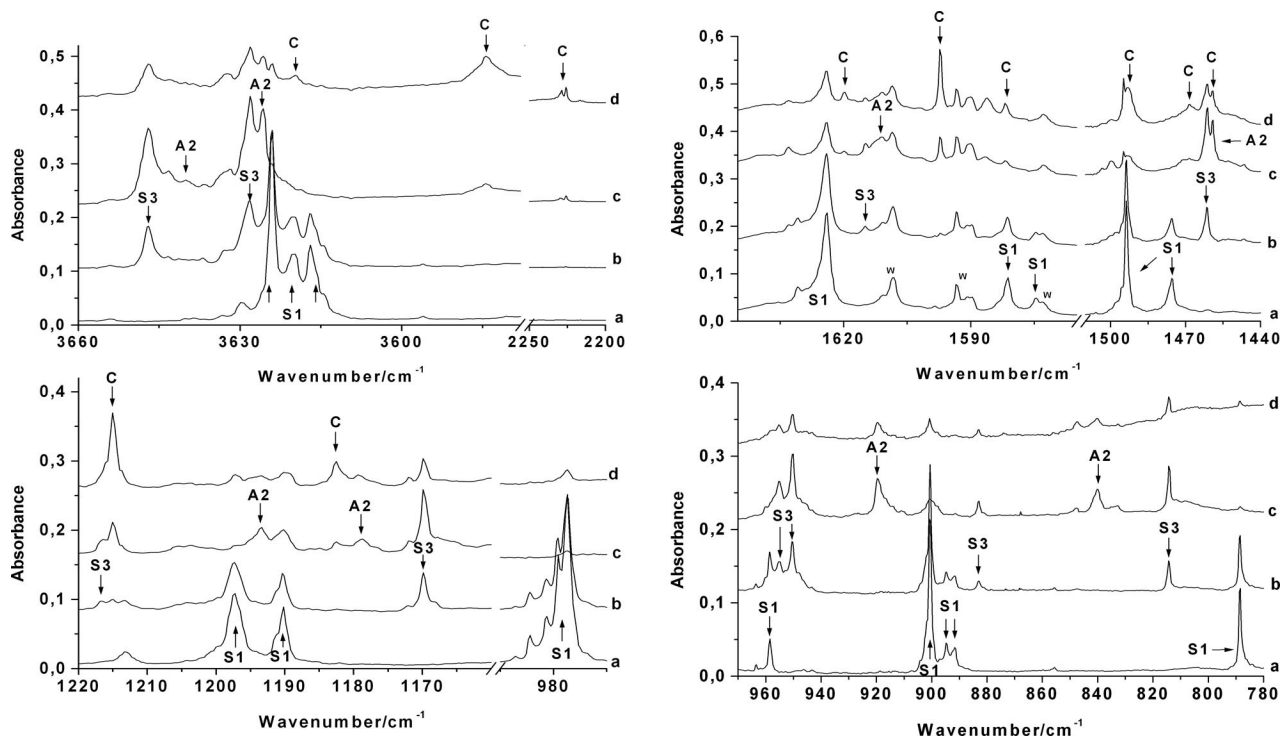


Figure 1. The 3660–2200, 1640–1440, 1220–970, and 970–780 cm^{-1} regions in the spectra of salicylaldehyde/Ar matrix recorded directly after matrix deposition (a), after its irradiation for 2 and 90 min with $\lambda > 320$ nm (b and c, respectively) followed by irradiation with full output of a mercury lamp for 25 min (d). Bands labeled “w” are due to water contamination.

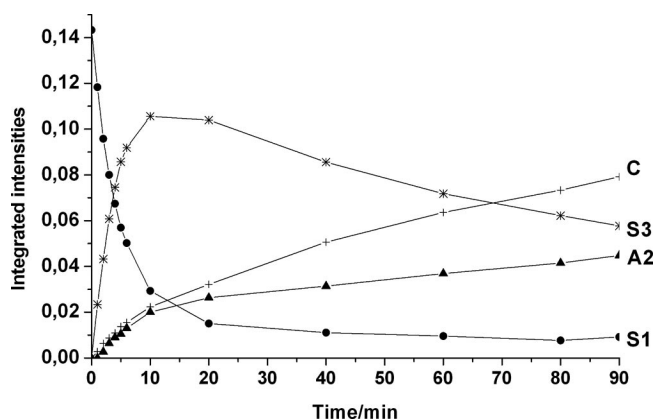


Figure 2. Time evolution of photoproducts S3, A2, and C and deposited salicylaldehyde sample S1 after photolysis of salicylaldehyde/Ar matrix at 11 K with the filtered mercury lamp radiation $\lambda > 320$ nm. Integrated intensities of the absorptions at 788.6, 814.2, and 840.1 cm^{-1} were used for salicylaldehyde conformers S1, S3, and A2, respectively, and integrated intensity of the absorption at 1215.0 cm^{-1} was used for photoproduct C.

ferent conformers of the salicylaldehyde molecule. The assignment of the three sets of frequencies to the particular conformer will be discussed further. The most characteristic bands of product C appeared in the regions of the OH

(3716.6, 3620.4, 3584.4 cm^{-1}) and $\text{C}\equiv\text{N}$ stretching vibrations (2228.8, 2226.0 cm^{-1}). The 3716.6 and 3620.4 cm^{-1} frequencies suggest that water is the photoreaction product. The dehydration of salicylaldehyde may lead to the formation of 2-cyanophenol, which was postulated to be a minor photolysis product in irradiated hexane and aqueous base solution of salicylaldehyde.^[19] The comparison of the frequencies characteristic for C with the reported infrared spectra of 2-cyanophenol^[30,31] confirms, indeed, formation of the latter molecule in the studied photoreaction. The water and 2-cyanophenol molecules are both proton donors and acceptors, so, being trapped in the same matrix cage after salicylaldehyde is photodissociated, they may form a hydrogen-bonded complex. On the basis of the experimental data, product C was tentatively identified as the 2-cyanophenol– H_2O hydrogen bonded complex. The performed calculations for the 2-cyanophenol– H_2O complexes support this conclusion. In Table 2 the experimental frequencies identified for product C are compared with the calculated frequencies for the 2-cyanophenol– H_2O complex and with the reported experimental frequencies for 2-cyanophenol.^[30,31] DFT/B3LYP/6-311++G(2d,2p) calculations resulted in a number of stable structures for the 2-cyanophenol– H_2O complexes. The seven most stable structures of the 2-cyanophenol– H_2O complex (in three structures the cy-

Table 1. Comparison of the observed and calculated frequencies (cm^{-1}) for the three salicylaldehyde conformers (*syn1*, *syn3*, and *anti2*) identified in argon matrices. The DFT/B3LYP/6-311++G(2d,2p) calculated anharmonic frequencies are presented, the intensities (km mol^{-1}) correspond to their harmonic counterparts. The approximate assignment is given on the basis of the calculated PED.^[a]

S1, <i>syn1</i>				S3, <i>syn3</i>				A2, <i>anti2</i>				Approximate Assignment
$\nu_{\text{obsd.}}$	$f^{[b]}$	$\nu_{\text{calcd.}}$	$I_{\text{calcd.}}$	$\nu_{\text{obsd.}}$	I	$\nu_{\text{calcd.}}$	$I_{\text{calcd.}}$	$\nu_{\text{obsd.}}$	I	$\nu_{\text{calcd.}}$	$I_{\text{calcd.}}$	
3624.1	vs	3659	146	3647.0	s	3664	65	3640.1	w	3637	66	ν_{OH}
3258 - 3195	vs	3185	258	3627.9	vs	3664	149	3625.6	vs	3634	142	$\nu_{\text{OH}_{\text{HB}}}$, ν_{OH}
1630.9	w	1638	21	1633.0	w	1647	11			1644	7	$\nu_{\text{CN}}+\delta(\text{NCH}+\text{CCH})$
				1503.1	vw	1498	15					$\delta\text{CCH}_{\text{ring}}+\nu_{\text{CC}_{\text{ring}}}$
1493.7	s	1494	40									$\delta\text{CCH}_{\text{ring}}+\delta\text{COH}$
1475.6	w	1470	51									$\nu_{\text{CC}_{\text{ring}}}+\delta\text{CCH}_{\text{ring}}+\nu_{\text{CO}}$
				1461.4	s	1459	65	1459.3	s	1461	54	$\delta\text{CCH}_{\text{ring}}+\nu_{\text{CC}_{\text{ring}}}$
				1417.5	vw	1415	28					$\delta\text{NOH}+\delta\text{COH}+\delta(\text{NCH}+\text{NCC})$
				1404.8	s	1415	28					$\delta(\text{NCH}+\text{NCC})+\delta\text{NOH}$
								1301.1	w	1302	39	$\nu_{\text{CC}_{\text{ring}}}+\delta\text{CCH}_{\text{ring}}$
1396.5	vw	1394	59									$\delta\text{COH}+\delta\text{CCH}_{\text{ring}}+\delta(\text{NOH})$
				1322.9	m	1329	49					$\nu_{\text{CC}_{\text{ring}}}+\delta\text{COH}+\delta\text{CCH}_{\text{ring}}$
										1377	13	$\delta(\text{NCH}+\text{NCC})+\delta\text{NOH}$
1318.0	vw	1313	14	1302.4	m	1302	15					$\nu_{\text{CC}_{\text{ring}}}+\delta\text{CCH}_{\text{ring}}$
1273.3	vs	1280	62	1272.2	s	1280	93	1325.0	m	1325	86	$\delta\text{NOH}+\delta(\text{NCH}+\text{NCC})$
				1269.8								
								1320.0	w	1333	48	$\delta\text{CCH}_{\text{ring}}+\nu_{\text{CC}_{\text{ring}}}+\delta\text{COH}$
				1248.6	s	1240	66	1250.1	m	1235	98	$\nu_{\text{CO}}+\delta\text{NOH}+\delta\text{CCC}_{\text{ring}}$
1197.3	m	1203	43	1216.5	vw	1209	28	1193.5	w	1188	36	$\nu_{\text{CO}}+\nu_{\text{CC}_{\text{ring}}}+\delta(\text{NCH}+\text{NCC})$
				1169.8	m	1174	55	1190.5	w	1183	84	$\nu_{\text{CC}(\text{N})}+\nu_{\text{CC}_{\text{ring}}}+\delta(\text{NCH}+\text{NCC})$
				1094.9	m	1096	57	1190.5	w	1183	84	$\delta\text{COH}+\delta\text{CCH}_{\text{ring}}$
				1094.9	m	1096	57	1090.1	w	1096	31	$\nu_{\text{CC}_{\text{ring}}}+\delta\text{CCH}_{\text{ring}}$
977.3	s	974	153	950.3	m	956	207	919.2	w	908	171	$\nu_{\text{NO}}+\delta(\text{NCH}+\text{NCC})$
900.6	m	898	54	883.1	vw	878	38					$\delta\text{CCC}_{\text{ring}}+\delta(\text{NCH}+\text{NCC})$
788.6	w	790	15	814.2	w	817	37	840.1	vw	837	58	$\nu_{\text{CC}_{\text{ring}}}+\nu_{\text{CO}}+\delta\text{CCC}_{\text{ring}}$
753.2	s	757	48	751.5	s	765	60	753.0	s	767	64	$\gamma_{\text{CCH}_{\text{ring}}}+\gamma_{\text{CCCO}}+\tau_{\text{CCCC}_{\text{ring}}}$
686.9	vw	679	109									τ_{COH}
650.9	m	657	36	631.3	w	640	24					$\delta\text{CCC}_{\text{ring}}+\delta(\text{NCC}+\text{NCH}+\text{CCH})$

[a] PEDs for *syn1*, *syn3*, and *anti2* isomers are presented in Tables S2–S4 (Supporting Information). [b] Relative experimental intensities: vs – very strong, s – strong, m – medium, w – weak, vw – very weak.

Table 2. Comparison of the observed and calculated frequencies (cm^{-1}) for the 2-cyanophenol– H_2O and 2-[D_1]cyanophenol–HDO complexes identified in argon matrices. The DFT/B3LYP/6-311++G(2d,2p) calculated harmonic and anharmonic frequencies are presented; the intensities (kmol^{-1}) correspond to the harmonic frequencies. The approximate assignment is given on the basis of the calculated potential energy distribution (PED).^[a]

2-Cyano-phenol ^[30]	2-Cyanophenol– H_2O					2-[D_1]cyanophenol–HDO				Approximate description
	Experimental		Calculated			Experimental		Calculated		
	$\nu_{\text{obsd.}}$	$I^{[b]}$	ν_{harm}	I	ν_{anharm}	$\nu_{\text{obsd.}}$	I	ν_{harm}	I	
3586	3716.6	s	3903	109	3708	3685.6, 3696.8	m	3878	47	$\nu\text{OH}(\text{H}_2\text{O})/\nu\text{OH}(\text{HDO})$
	3620.4	w	3786	49	3605	2648.1	w	2770	58	$\nu\text{OH}(\text{H}_2\text{O})/\nu\text{OD}(\cdot\text{DO})$
2223	3584.4	s	3778	77	3577	2599.2, 2585.4	m	2750	49	$\nu\text{OH}/\nu\text{OD}$
	2228.8, 2226.0	vs.	2298	94	2268	2228.7, 2226.0	w	2298	94	$\nu\text{C}=\text{N} + \nu\text{C}-\text{C}(\text{N})$
1603	1620.0	m	1652	36	1608	1614.7	vw	1646	55	$\nu\text{CC}_{\text{ring}} + \delta\text{CCH}_{\text{ring}} + \delta\text{CCC}_{\text{ring}}$
	1597.2	vs	1644	108	1584	1399.3	s	1432	67	$\delta\text{H}_2\text{O}/\delta\text{HDO}$
1590	1581.8	m	1611	43	1555	1581.8	vw	1606	27	$\nu\text{CC}_{\text{ring}} + \delta\text{CCH}_{\text{ring}}$
	1506	s	1520	73	1482	1494.8, 1492.7	vs	1519	75	$\delta\text{CCH}_{\text{ring}} + \nu\text{CC}_{\text{ring}}$
1368	1468.4	w	1498	31	1462	1460.5	s	1491	40	$\delta\text{CCH}_{\text{ring}} + \nu\text{CC}_{\text{ring}}$
	1275	w	1377	23	1340					$\delta\text{CCH}_{\text{ring}} + \nu\text{CC}_{\text{ring}} + \delta\text{COH}$
1246	1307.0	m	1331	26	1301					$\nu\text{CC}_{\text{ring}} + \nu\text{CO} + \delta\text{CCH}_{\text{ring}}$
	1215	w	1277	29	1248	1259.5, 1253.0	w	1274	64	$\nu\text{CC}_{\text{ring}} + \nu\text{CO} + \delta\text{CCH}_{\text{ring}}$
1182	1215.0	vs	1243	132	1204					$\delta\text{COH} + \delta\text{CCH}_{\text{ring}} + \nu\text{C}-\text{C}(\text{N})$
	1160	m	1201	29	1176					$\delta\text{CCH}_{\text{ring}} + \nu\text{CC}_{\text{ring}} + \delta\text{COH}$
1104	1150.1	m	1180	35	1164	1178.6	vw	1183	10	$\delta\text{CCH}_{\text{ring}} + \nu\text{CC}_{\text{ring}}$
	1034	w	1052	10	1035	1115.7	w	1138	25	$\delta\text{CCC}_{\text{ring}} + \nu\text{CC}_{\text{ring}} + \delta\text{CCH}_{\text{ring}}$
847	936.5	vs	960	87	936.5	936.5	vs	960	87	$\nu\text{CC}_{\text{ring}} + \delta\text{CCH}_{\text{ring}}$
	847	w	860	11	844					$\delta\text{COD} + \delta\text{CCC}_{\text{ring}}$
767	762.2, 765.3	s	776	63	769	762.0	s	776	67	$\delta\text{CCC}_{\text{ring}}$
	732	vw	748	0	762					γCCH
										$\tau\text{CCCC}_{\text{ring}}$

[a] PEDs for the 2-cyanophenol– H_2O and 2-cyanophenol–HDO complexes are presented in Tables M9, M10. [b] Relative experimental intensities; vs – very strong, s – strong, m – medium, w – weak, vw – very weak.

nophenol has the *s-cis* conformation and in the other four the *s-trans* one), their corresponding interaction energies, and their calculated vibrational frequencies are presented in the Supporting Information (Figure S4; Tables S11 and S12). There are small differences between the frequencies calculated for the optimized sets of structures; most information concerning the structure of the complexes is provided by the three OH stretching vibrations. The relatively low value of the frequency identified for the (C)OH stretching vibration of 2-cyanophenol (3584.4 cm^{-1}) indicates that the *s-cis* 2-cyanophenol isomer is present in the matrix with a weak intramolecular hydrogen bond. From the three optimized structures of the *s-cis* 2-cyanophenol complex the one in which the (C)OH group serves as a proton donor toward water molecule can be safely rejected as the (C)OH stretching frequency in this complex is expected to have much lower value (3222 cm^{-1}) than the identified frequency (3584.4 cm^{-1}) of the complex present in the matrix. The two identified water stretching vibrations ($3716.6, 3584.4\text{ cm}^{-1}$) indicate that water serves as a proton donor in the complex. Unfortunately, the obtained experimental set of frequencies does not allow us to conclude whether water is attached to the $\text{C}\equiv\text{N}$ group or to the oxygen atom of the (C)OH group; the two structures that are presented in Figure 3 are characterized by very similar sets of frequencies. In Table 2 the frequencies identified for product C are compared with those calculated for the complex in which water serves as a proton donor toward the $\text{C}\equiv\text{N}$ group of salicylaldehyde.

In the Supporting Information (Table S8), the selected structural parameters for the two complexes are presented and their calculated frequencies are collected (Tables S9 and S10).

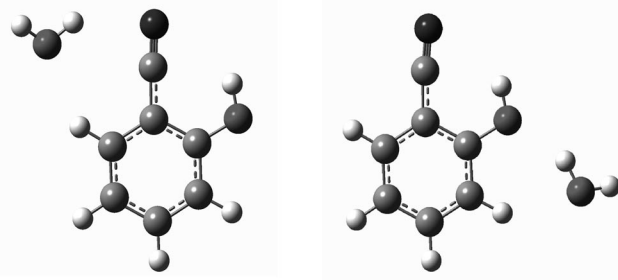


Figure 3. The structures of the 2-cyanophenol– H_2O complexes that are possibly formed after photodissociation of salicylaldehyde. The structures were optimized by DFT/B3LYP/6-311++G(2d,2p) calculations.

No absorptions characteristic for benzoxazole^[32] were identified in the spectra of the irradiated matrices; benzoxazole was reported to be the major photolysis product of salicylaldehyde in aqueous solutions.^[18]

Photochemistry of [D_2]Salicylaldehyde

In the spectra of the irradiated matrices doped with [D_2]salicylaldehyde the counterparts of the four sets of bands,

S1, S3, A2, and C, observed in the spectra of the hydrogenated samples were identified. As already mentioned, the S1, S3, and A2 bands are assigned to the three salicylaldoxime conformers. In the Supporting Information the spectra of $[D_2]$ salicylaldoxime/Ar matrices are shown (Figure S2) and the frequencies of the S1, S3, and A2 conformers identified for $[D_2]$ salicylaldoxime are compared with their counterparts in salicylaldoxime (Tables S2–S4). The band set C corresponding to the 2-cyanophenol– H_2O complex shows some interesting features. The deuterium counterparts of the 3584.4 cm^{-1} $\nu(\text{OH})$ and 1215.0 cm^{-1} $\delta(\text{COH})$ vibrations of 2-cyanophenol are identified at 2599.2 and 938.4 cm^{-1} , respectively, in the spectra of 2- $[D_1]$ cyanophenol (that is formed from $[D_2]$ salicylaldoxime) as expected. The frequencies of the bonded water molecule are identified at 3685.6 , 3696.8 , 2648.1 , and 1399.3 cm^{-1} , which evidences the formation of HDO molecule in the experiment with $[D_2]$ salicylaldoxime. The 3685.6 , 3696.8 cm^{-1} doublet corresponds to the OH stretch, the 2648.1 cm^{-1} band to the OD stretch, and the 1399.3 cm^{-1} one to the HDO bend. The 2648.1 cm^{-1} band is a counterpart of the 3620.4 cm^{-1} absorption in the spectra of the nondeuterated sample, which indicates that the OD group of the HDO molecule acts as a proton donor in the 2-cyanophenol–HDO complex. The 2648.1 cm^{-1} band is shifted ca. 62 cm^{-1} toward lower frequencies with respect to the corresponding vibration of the nonperturbed HDO molecule (observed at ca. 2710 cm^{-1}),^[33] whereas the 3685.6 , 3696.8 cm^{-1} doublet has very close frequencies to the OH stretch of nonperturbed HDO (ca. 3687 cm^{-1}).^[33]

Conformational Analysis

The performed DFT/B3LYP/6-311++G(2d,2p) calculations resulted in 16 true minima on the potential energy surface of salicylaldoxime. The structures of all 16 optimized conformers, their energies, and calculated vibrational frequencies are presented in the Supporting Information (Figure S1, Tables S5 and S6). The calculations were also performed by the MP2/6-311++G(2d,2p) method that resulted in similar structures and their corresponding energy values like those performed by DFT method (Figure S1). The three salicylaldoxime conformers that are identified in the spectra of the studied matrices are depicted in Figure 4. In Table 1 the observed frequencies for the three conformers are compared with the theoretical ones.

In the Supporting Information (Tables S1–S4), selected structural parameters and the full sets of calculated frequencies for the three conformers are collected. The theoretical relative abundances (calculated from the Gibbs free energies at 298 K) of the three conformers in the gas phase, in selected nonpolar and polar solutions, are shown in Table 3; the calculated abundances for all conformers are presented in the Supporting Information (Table S7).

The global minimum corresponds to a *syn1* conformer in which the C(N)–H and N–O bonds are in the eclipsed position and the (C)OH group forms an intramolecular hy-

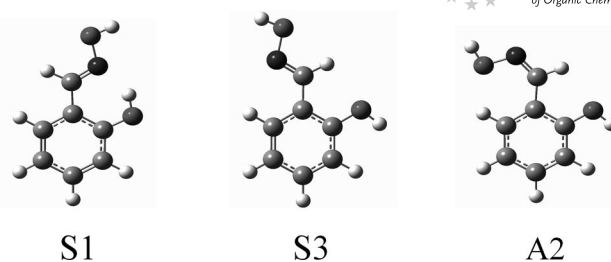


Figure 4. The DFT/B3LYP/6-311++G(2d,2p) optimized structures of the three salicylaldoxime conformers identified in the matrices.

Table 3. The abundances of the most populated conformers of salicylaldoxime in various environments.

Environment	<i>syn1</i>	<i>syn3</i>	<i>anti2</i>
Solid argon	99.9	0.0	0.0
Heptane	99.5	0.3	0.0
Cyclohexane	99.4	0.1	0.0
Water	57.2	38.4	0.5
Acetonitrile	60.8	35.9	0.5
Ethanol	65.0	32.2	0.5

drogen bond with the nitrogen atom. The experimental frequencies observed in the spectra recorded directly after matrix deposition (set S1) show a very good agreement with the theoretical ones calculated for the *syn1* conformer (Table 1), which evidences the presence of the *syn1* isomer in the matrix. The observed splitting of the S1 bands (Figure 1, Table S2) is due to site effects as evidenced by the different splitting pattern of the S1 bands in the spectra of argon and nitrogen matrices. The spectra of salicylaldoxime in argon and nitrogen matrices are presented in Figure S3 (Supporting Information). No other salicylaldoxime conformers were detected in the spectra of the matrices recorded directly after deposition, which is in accord with the calculated abundance of *syn1* equal to ca. 100% in neutral environment. It is known that the conformational populations characteristic of the gaseous equilibria prior to deposition is preserved in the matrix if the barriers between various conformers are relatively high.^[34] The presence of the intramolecular hydrogen bond is manifested in the spectra of *syn1* salicylaldoxime first of all by appearance of a strong broad absorption in the $3258\text{--}3195\text{ cm}^{-1}$ region due to the OH stretching vibration in the (C)O–H \cdots N bond (Supporting Information, Figure S3). The band is shifted ca. 400 cm^{-1} toward lower frequencies as compared to the corresponding band of the nonbonded OH group. The low frequency shift of the $\nu(\text{OH})$ frequency is accompanied by a shift of the COH in-plane and out-of-plane bending vibrations toward higher frequencies with respect to the corresponding vibrations of the nonbonded COH group. The OH out-of-plane vibration appears at 686.9 cm^{-1} , and the COH in-plane internal coordinate contributes to the three normal modes observed at 1493.7 , 1417.5 , and 1396.5 cm^{-1} . As can be seen in Table 1 the vibrations of the internal coordinates are strongly coupled, two or more internal coordinates give contribution to the potential energy of the normal modes of *syn1* (with the exception of the modes charac-

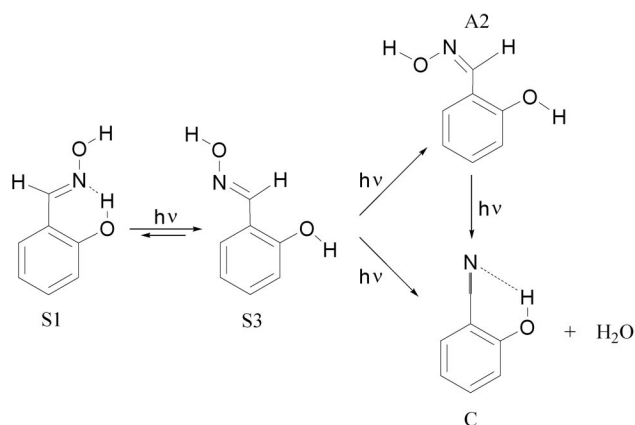
terized by 3624.1, 686.9 cm^{-1} frequencies). The strong coupling of the internal modes is also manifested in the spectrum of the *syn1* conformer of the $[\text{D}_2]$ salicylaldoxime molecule. In the Supporting Information (Table S2) the experimental frequencies of *syn1* of $[\text{D}_2]$ salicylaldoxime are compared with the calculated ones for this molecule; the agreement of the two sets of frequencies gives additional support for the correct identification of the conformer present in the matrix after deposition. Matrix irradiation leads to conversion of *syn1* into two other conformers of salicylaldoxime. The disappearance of the 3258–3195 cm^{-1} absorption characteristic for the hydrogen bond in the *syn1* conformer and growth of the bands in the region of the vibrations of nonbonded OH group indicates that the hydrogen bond dissociates during irradiation. Comparison of the experimental frequencies for product S3 with the theoretical ones calculated for the optimized conformers without an internal hydrogen bond suggests two possible structures for product S3, namely, *syn3* (Figure 4) and *syn4* (Figure S1, Supporting Information). In *syn3*, the C(H)NOH group is turned around the C–C(N) bond by 180° and simultaneously the (C)OH group is turned around the C–C bond also by 180° with respect to *syn1*, whereas in *syn4* only the C(H)NOH group is rotated. The differences in frequencies between *syn3* and *syn4* triggered by rotation of the OH group are very small (Tables S2 and S5, Supporting Information). However, careful comparison of the observed frequencies for product S3 with the calculated ones for the *syn3* and *syn4* conformers led us to the conclusion that product S3 can be identified as the *syn3* salicylaldoxime although the presence of *syn4* in the studied matrices cannot be excluded. In Table 1 the identified frequencies for product S3 are compared with the calculated ones for the *syn3* conformer; as one can see, the agreement between the experimental and calculated frequencies is very good. In the irradiated matrices doped with partially deuterated sample, the *syn3* $[\text{D}_2]$ salicylaldoxime conformer was identified and characterized spectroscopically. The identified frequencies of partially deuterated *syn3* $[\text{D}_2]$ salicylaldoxime are in accord with the calculated ones for this species (Table S3, Supporting Information), which provides additional evidence for the correctness of the identification of product S3. Product A2 is safely identified as *anti2* salicylaldoxime (Figure 4). In *anti2* salicylaldoxime, the NOH group is rearranged with respect to the C=N bond as compared to the *syn3* conformer. This is reflected in different frequencies of the normal modes of the two isomers to which the internal coordinates of the C(H)NOH group give contribution. For example, the normal modes corresponding to the coupled $\nu(\text{NO}) + \delta(\text{NCH} + \text{NCC})$ internal coordinates are identified at 950.3 cm^{-1} in *syn3* and at 919.2 cm^{-1} in *anti2* salicylaldoxime conformers. In Table 1, the identified frequencies for product A2 are compared with the calculated ones for *anti2* salicylaldoxime and in the Supporting Information (Table S4), the frequencies identified for A2 in experiment with $[\text{D}_2]$ salicylaldoxime are compared with the theoretical ones for the *anti2* $[\text{D}_2]$ salicylaldoxime molecule. For both the hydrogenated and partially deuterated salicylaldoxime

molecules a good agreement between the experimental and theoretical frequencies is observed, which evidences the correctness of the identification of the A2 product.

Mechanism of Reaction

The analysis of the spectra recorded after matrix deposition evidences that the salicylaldoxime molecule trapped in the matrix has the *syn1* conformation with an intramolecular hydrogen bond. This is in accord with the results of the calculations that indicate the *syn1* conformer to be the most stable one among all optimized structures, with the abundance close to 100% in neutral environment (Table 3). The graph presented in Figure 2 demonstrates that irradiation of the matrix with $\lambda > 320$ nm leads to the photoconversion of the *syn1* conformer into the *syn3* conformer of salicylaldoxime, which is the primary product. In the *syn3* conformer, the C(H)NOH and (C)OH groups are rotated by 180° around the C–C and C–O bonds, respectively, as compared to their arrangement in *syn1* salicylaldoxime. The yields of the other two products: *anti2* salicylaldoxime and 2-cyanophenol– H_2O complex, increase noticeably with an increase in the *syn3* salicylaldoxime concentration in the matrix. The structure of the *anti2* conformer as well as its growth curve during matrix irradiation indicate that it is formed as a secondary product from the *syn3* conformer. The conversion *syn3*–*anti2* salicylaldoxime requires a rearrangement of the NOH group with respect to the C=N bond. The *syn*–*anti* isomerization of oximes has been extensively studied both experimentally and theoretically;^[35] it was found that the isomerization may proceed through a rotation or inversion mechanism or a mixture of both. However, it cannot be excluded that in the performed experiment the *anti2* isomer is formed in recombination reaction of Ph(OH)C(H)N and OH radicals, as discussed later. During prolonged matrix photolysis with $\lambda > 320$ nm radiation, the yield of the 2-cyanophenol– H_2O complex increases at the expense of *syn3* salicylaldoxime. When the matrix is photolyzed with the full output of the mercury lamp the yield of the 2-cyanophenol– H_2O complex strongly increases at the expense of both the *syn3* and *anti2* conformers (Figure 1). The photochemical reactions observed in the studied matrices are summarized in Scheme 1.

The experiment with $[\text{D}_2]$ salicylaldoxime, in which the 2- $[\text{D}_1]$ cyanophenol–HDO complex is produced, indicates that the water molecule is formed in a dehydration reaction of the C(H)NOH group. This hypothesis is supported by the photodissociation studies of simple oximes in the gas phase.^[36–39] Flash photolysis studies of oximes with transient absorption detection under isothermal and adiabatic conditions evidenced that the predominant primary photochemical reaction in the gas phase is the formation of OH and $\text{R}_1\text{R}_2\text{CN}$ radicals.^[36] The photodissociation study of acetaldoxime led to the conclusion that the singlet $^1(\pi, \pi^*)$ excited acetaldoxime undergoes intersystem crossing to the triplet state, followed by dissociation to generate the $\text{CH}_3\text{C}=\text{N}$ and OH radicals.^[38] A similar photodissociation



Scheme 1.

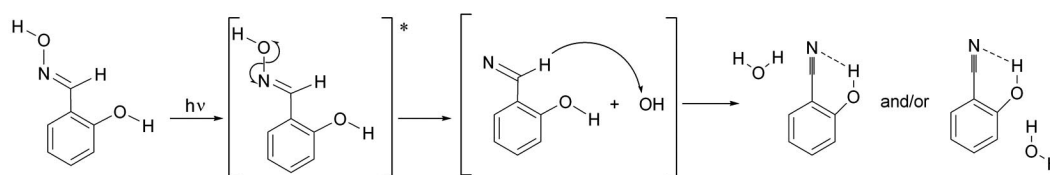
process may occur for salicylaldehyde, leading to the formation of the Ph(OH)C(H)N and OH radicals. The OH and the Ph(OH)C(H)N radicals trapped in the same cage may produce *anti2* or *syn1* conformers of salicylaldehyde or OH may abstract a hydrogen atom from the CH group of Ph(OH)C(H)N to form H_2O and 2-cyanophenol. The two molecules trapped in the same cage form a complex. Scheme 2 presents the reaction channel leading to a formation of the 2-cyanophenol– H_2O complex.

As already mentioned in the Introduction, earlier studies^[18,19] indicate that the major result of salicylaldehyde photolysis in polar solvents like water or ethanol and non-polar ones like hexane or pentane is cyclization to give benzoxazole. Photohydrolysis reaction leading to the formation of salicylaldehyde is a minor reaction channel, however, may become important in the acidified solutions. Ferris and Antonucci reported also 2-cyanophenol to be the minor photoproduct of salicylaldehyde photolysis in hexane solutions; however, the mechanism of this reaction was not proposed. No benzoxazole was detected in our experiments, which is in accord with an earlier proposed mechanism of its formation in solutions through the excited phenolate anion;^[18,19] the phenolate anion cannot be formed in the cryogenic matrices under the conditions of our experiment. However, according to Haley and Yates, the mechanism with the phenolate ion as an intermediate applies only to the conformer(s) with intermolecular hydrogen bonds, and for the conformer with an intramolecular hydrogen bond the authors proposed a more complicated mechanism with a direct transfer of the hydroxy proton to the nitrogen atom and formation of a zwitterion in a first step; the zwitterion reacts further to form benzoxazole. The authors con-

cluded that in solution both conformers with intra- and intermolecular hydrogen bonds exist. In the gas phase and in nonpolar solvents, the abundance of the *syn1* salicylaldehyde conformer is close to 100%, whereas in polar solvents the abundance of the *syn3* conformer increases to ca. 32–38% at the expense of the *syn1* conformer (see Table 3). The summarized abundance of all other conformers is below 2.5%. So, the calculations confirm the existence of an equilibrium between the conformers with and without intramolecular hydrogen bonds in polar solvents. The performed experimental studies suggest however that the first step in the photochemical reaction of the *syn1* salicylaldehyde conformer in solution may be its conversion into the *syn3* conformer in which the intramolecular hydrogen bond is replaced by intermolecular hydrogen bonds with the solvent molecules. The yield of this reaction will strongly depend on the type of solvent and on the solvation shell of the salicylaldehyde molecule.

Conclusions

The FTIR matrix isolation and DFT/B3LYP/611++G(2d,2p) study of salicylaldehyde indicate that the most stable *syn1* conformation stabilized by an intramolecular $(\text{C})\text{O}-\text{H}\cdots\text{N}$ hydrogen bond is trapped in an argon matrix. The irradiation of the matrix with $\lambda > 320$ nm leads to the conversion of the *syn1* conformer into the *syn3* conformer in which the C(H)NOH and $(\text{C})\text{OH}$ groups are turned by 180° around the $\text{C}-\text{C}$ and $\text{C}-\text{O}$ bonds, respectively, and the intramolecular hydrogen bond is broken. The *syn3* salicylaldehyde reacts further along one of the three pathways, including *syn3*→*anti2* isomerization reaction, dissociation of *syn3* salicylaldehyde into 2-cyanophenol and water, or conversion reaction of *syn3* back to *syn1*; regeneration of the *syn1* conformer gives very small contribution to the overall reaction. After prolonged photolysis with $\lambda > 320$ nm radiation or with the full output of the mercury lamp, both the *syn3* and *anti2* conformers photodissociate to give 2-cyanophenol and water, which form a 2-cyanophenol– H_2O complex. The experiments with partially deuterated $[\text{D}_2]$ salicylaldehyde provide information on the mechanism of formation of the 2-cyanophenol– H_2O complex. Salicylaldehyde photodissociates into Ph(OH)HC=N and OH radicals, then the OH radical abstracts a hydrogen atom from Ph(OH)HC=N to produce 2-cyanophenol and water that form a hydrogen-bonded complex. Recombination of Ph(OH)HC=N and OH radicals may also lead to the formation of the *syn1* and *anti2* conformers. The ob-



Scheme 2.

tained results also suggest that in solution the photolytic conversion of the *syn1* and *syn3* conformers (with and without intramolecular hydrogen bond) into benzoxazole may occur by the same mechanism of phenolate ion formation. However, in the case of the *syn1* conformer with the intramolecular hydrogen bond, a first step of an overall reaction is *syn1*→*syn3* conversion.

Experimental Section

Infrared Matrix Isolation Studies: The salicylaldehyde/argon(nitrogen) matrices were obtained by simultaneous deposition of vapor above solid salicylaldehyde kept at 318 K and argon on a gold-plated copper mirror kept at 11 K by a closed cycle helium refrigerator (Air Products, Displex 202 A). The matrix concentration was controlled by the matrix gas flow rate that was adjusted to minimize the concentration of salicylaldehyde dimers and higher aggregates. The salicylaldehyde/argon matrices were irradiated with the output of the mercury lamp. After the infrared spectra of the initial deposits have been recorded, the samples were subjected to the filtered radiation of a 200 W medium pressure mercury lamp (Phillips CS200W2). A 5 cm water filter served to reduce the amount of infrared radiation reaching the matrix; the glass long-wavelength pass filters (Zeiss WG 320, Zeiss WG 305) were applied to cut off the radiation with $\lambda < 320$ or 305 nm; in some experiments the matrices were irradiated with the full output of mercury lamp. Salicylaldehyde was obtained from Aldrich with specified purity 98%. The partially deuterated [D₂]salicylaldehyde was obtained by dissolving salicylaldehyde in D₂O and evaporating the heavy water, the procedure was repeated three times. The matrices were prepared in the same way as for the nondeuterated sample. The infrared spectra (resolution 0.5 cm⁻¹) were recorded in a reflection mode with Bruker 113v FTIR spectrometer by using a MCT detector cooled by liquid N₂.

Computational Methods: Optimization of all the structures as well as calculation of harmonic and anharmonic vibrational spectra were performed with the Gaussian03 suite of programs.^[40] DFT/B3LYP/6-311++G(2d,2p) calculations were done to optimize the structures and to calculate the harmonic and anharmonic frequencies. The MP2/6-311++G(2d,2p) method has also been applied to optimize the structures of salicylaldehyde conformers however only the harmonic frequencies were calculated by the MP2 method. For all energies the zero-point energy values have been considered. All the stationary points were unambiguously characterized as minima or transition states by their vibrational spectra. To investigate the effects of a polar environment on the structure and energetics of the salicylaldehyde conformers the Conductor-like Polarizable Continuum Model (CPCM) at the B3LYP/6-311++G(2d,2p) levels was applied. A potential energy distribution (PED) of the normal modes was computed in terms of natural internal coordinates with the Gar2ped program.^[41]

Supporting Information (see footnote on the first page of this article): Optimized structures of 16 salicylaldehyde conformers and 7 2-cyanophenol–H₂O complexes; calculated vibrational frequencies for all optimized salicylaldehyde conformers and all optimized 2-cyanophenol–H₂O complexes; experimental infrared spectra of [D₂]salicylaldehyde matrices; selected structural parameters and comparison of experimental frequencies with theoretical ones for the 3 salicylaldehyde and [D₂]salicylaldehyde conformers and 2 2-cyanophenol–H₂O and 2-[D₁]cyanophenol–HDO complexes identified in the present study.

- [1] S. R. Sandler, W. Karo, *Organic Functional Group Preparation*, Academic Press, San Diego, CA, **1989**; R. Kim, H. G. Lee, E. J. Kim, S. G. Lee, Y. J. Yoon, *J. Org. Chem.* **2010**, *75*, 484–486 and references cited therein; W. Tang, A. Capacci, M. Sarvestani, X. Wei, N. K. Yee, Ch. H. Senanayake, *J. Org. Chem.* **2009**, *74*, 9528–9530.
- [2] G. W. Milne, *CRC Handbook of Pesticides*, CRC Press, Boca Raton, FL, **1995**.
- [3] E. B. Nielsen, P. D. Suzdak, K. E. Andersen, L. J. S. Knutsen, U. Sonnewald, C. Braestrup, *Eur. J. Pharmacol.* **1991**, *196*, 257–266.
- [4] D. M. Maxwell, C. N. Lieske, K. M. Brecht, *Chem. Res. Toxicol.* **1994**, *7*, 428–433.
- [5] A. M. Rush, J. R. Elliott, *Neurosci. Lett.* **1997**, *226*, 95–98.
- [6] M. Eddleston, L. Szinicz, P. Eyer, N. Buckley, *QJM* **2002**, *95*, 275–283.
- [7] K. Chalupský, P. Bartik, S. Eklová, G. Entlicher, *Gen. Physiol. Biophys.* **2003**, *22*, 233–242.
- [8] F. Jaroš, T. Straka, Z. Dobešová, M. Pintérová, K. Chalupský, J. Kuneš, G. Entlicher, J. Zicha, *Eur. J. Pharmacol.* **2007**, *575*, 122–126.
- [9] H. J. P. De Lijser, Ch.-K. Tsai, *J. Org. Chem.* **2004**, *69*, 3057–3067 and references cited therein.
- [10] S. Dhanya, H. P. Upadhyaya, A. Kumar, P. D. Naik, R. D. Saini, *J. Chem. Phys.* **2005**, *122*, 184322–184329 and references cited therein.
- [11] H. J. P. De Lijser, J. S. Kim, S. M. McGrorty, E. M. Ulloa, *Can. J. Chem.* **2003**, *81*, 575–585.
- [12] K. L. Cabbage, A. J. Orr-Ewing, K. I. Booker-Milburn, *Angew. Chem. Int. Ed.* **2009**, *48*, 2514–2517.
- [13] R. Alonso, P. J. Campos, M. A. Rodriguez, D. Sampedro, *J. Org. Chem.* **2008**, *73*, 2234–2239.
- [14] T. Stepanenko, L. Lapinski, M. J. Nowak, L. Adamowicz, *Vib. Spectrosc.* **2001**, *26*, 65–82.
- [15] a) E. J. Poziomek, *J. Pharm. Sci.* **1965**, *54*, 333–340; b) A. C. Pratt, J. H. Amin, P. de Mayo, *Tetrahedron Lett.* **1963**, *24*, 1585–1589; c) A. C. Pratt, Q. Abdul-Majid, *J. Chem. Soc. Perkin Trans. 1* **1986**, 1691–1693; d) I. Rico, M. T. Maurette, E. Oliveros, M. Riviere, A. Lattes, *Tetrahedron* **1980**, *36*, 1779–1783; e) Y. Takeda, H. Misawa, H. Sakuragi, K. Tokumaru, *Bull. Chem. Soc. Jpn.* **1989**, *62*, 2213–2218; f) T. Arai, Y. Furuya, H. Furuuchi, K. Tokumaru, *Chem Phys. Lett.* **1993**, *212*, 597–603.
- [16] H. Izawa, P. de Mayo, T. Tabata, *Can. J. Chem.* **1969**, *47*, 51–62.
- [17] M. F. Haley, K. Yates, *J. Org. Chem.* **1987**, *52*, 1817–1824.
- [18] M. F. Haley, K. Yates, *J. Org. Chem.* **1987**, *52*, 1825–1830.
- [19] J. P. Ferris, F. R. Antonucci, *J. Am. Chem. Soc.* **1974**, *96*, 2010; J. P. Ferris, F. R. Antonucci, *J. Am. Chem. Soc.* **1974**, *96*, 2014–2019.
- [20] K. H. Grellman, E. Tauer, *Tetrahedron Lett.* **1974**, *42*, 3707–3710.
- [21] C. H. Chang, T. L. Shieh, H. G. Floss, *J. Med. Chem.* **1977**, *20*, 176–178.
- [22] E. Kolehmainen, R. Gawinecki, B. Ośmiałowski, K. Trzebiałowska, *Magn. Reson. Chem.* **1997**, *35*, 778–784.
- [23] T. Bejoy, J. George, S. Sugunan, *Ind. Eng. Chem. Res.* **2009**, *48*, 660–670.
- [24] C. J. Milios, S. Piligkos, E. K. Brechin, *Dalton Trans.* **2008**, 1809–1817.
- [25] T. Irshaidat, *Tetrahedron Lett.* **2008**, *49*, 631–635.
- [26] J. Tshuma, Alarcón-Angeles, E. Palacios-Beas, R. Vargas-García, M. T. Ramírez-Silva, A. Rojas-Hernández, *Spectrochim. Acta Part A* **2007**, *66*, 879–883.
- [27] P. A. Wood, R. S. Forgan, D. Henderson, S. Parsons, E. Pidcock, P. A. Tasker, J. E. Warren, *Acta Crystallogr., Sect. B* **2006**, *62*, 1099–1111.
- [28] E. M. S. Maçôas, L. Khriachtchev, M. Petersson, R. Fausto, M. Räsänen, *J. Am. Chem. Soc.* **2003**, *125*, 16188–16189.

- [29] P. R. Schreiner, H. P. Reisenauer, F. C. Pickard IV, A. C. Simonetti, W. D. Allen, E. Mátyus, A. G. Császár, *Nature* **2008**, *453*, 906–909.
- [30] Y. I. Binev, M. K. Georgieva, L. I. Daskalova, *Spectrochim. Acta Part A* **2004**, *60*, 2601–2610.
- [31] M. Broquier, F. Lahmani, A. Zehnacker-Rentien, V. Brenner, P. Millié, A. Peremans, *J. Phys. Chem. A* **2001**, *105*, 6841–6850.
- [32] W. B. Collier, T. D. Klots, *Spectrochim. Acta A* **1995**, *51*, 1255–1272.
- [33] A. Engdahl, B. Nelander, *J. Phys. Chem.* **1985**, *89*, 2860–2864.
- [34] A. J. Barnes, *J. Mol. Struct.* **1984**, *113*, 161–174.
- [35] J. M. Lehn, *Chem. Eur. J.* **2006**, *12*, 5910–5915; F. Blanco, I. Alkorta, J. Elguero, *Croat. Chem. Acta* **2009**, *82*, 173–183 and references cited therein.
- [36] D. G. Horne, R. G. W. Norrish, *Proc. R. Soc. A* **1970**, *315*, 287–300.
- [37] P. J. Dagdigian, W. R. Andersen, R. C. Sausa, A. W. Miziolek, *J. Phys. Chem.* **1989**, *93*, 6059–6064.
- [38] P. Chowdhury, *J. Phys. Chem. A* **2002**, *106*, 10488–10493.
- [39] B. Nizamov, P. J. Dagdigian, *J. Phys. Chem. A* **2003**, *107*, 2256–2263.
- [40] M. J. Frisch, G. W. Trucks, H. B. Schlegel, G. E. Scuseria, M. A. Robb, J. R. Cheeseman, V. G. Zakrzewski, J. A. Montgomery Jr., R. E. Stratmann, J. C. Burant, S. Dapprich, J. M. Millam, A. D. Daniels, K. N. Kudin, M. C. Strain, O. Farkas, J. Tomasi, V. Barone, M. Cossi, R. Cammi, B. Mennucci, C. Pomelli, C. Adamo, S. Clifford, J. Ochterski, G. A. Petersson, P. Y. Ayala, Q. Cui, K. Morokuma, D. K. Malick, A. D. Rabuck, K. Raghavachari, J. B. Foresman, J. Cioslowski, J. V. Ortiz, A. G. Baboul, B. B. Stefanov, G. Liu, A. Liashenko, P. Piskorz, I. Komaromi, R. Gomperts, R. L. Martin, D. J. Fox, T. Keith, M. A. Al-Laham, C. Y. Peng, A. Nanayakkara, M. Challacombe, P. M. W.; B. Gill, Johnson, W. Chen, M. W. Wong, J. L. Andres, C. Gonzalez, M. Head-Gordon, E. S. Replogle, J. A. Pople, *Gaussian 98*, Revision A.8, Gaussian, Inc., Pittsburgh, PA, **1998**.
- [41] J. M. L. Martin, C. Van Alsenoy, *GAR2PED*, University of Antwerp, Antwerpen, Belgium, **1995**.

Received: March 14, 2010

Published Online: August 3, 2010